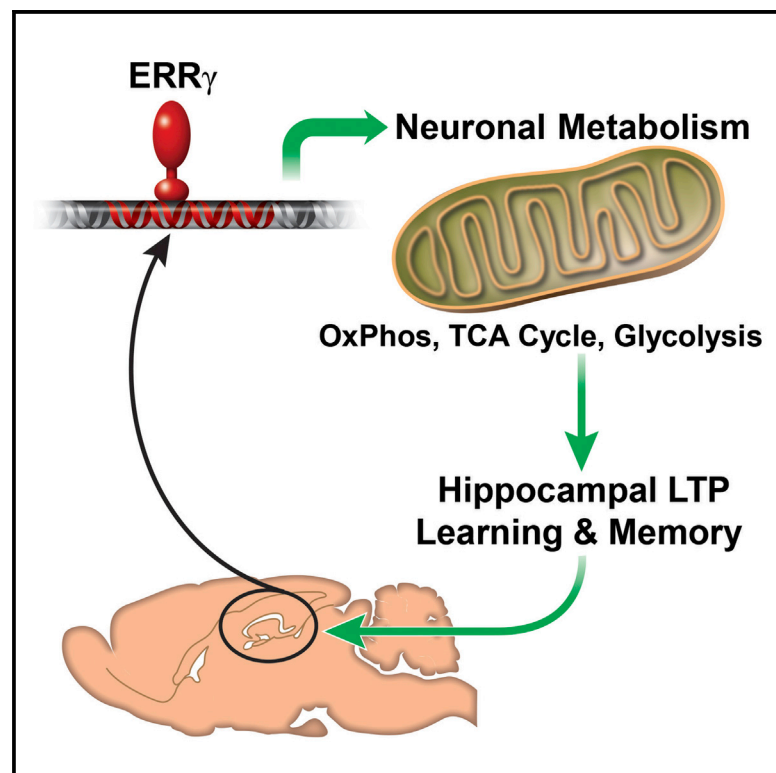


## Short Article

# Cell Metabolism

## Dependence of Hippocampal Function on $ERR\gamma$ -Regulated Mitochondrial Metabolism

### Graphical Abstract



### Authors

Liming Pei, Yangling Mu, ...,  
Fred H. Gage, Ronald M. Evans

### Correspondence

[lpei@mail.med.upenn.edu](mailto:lpei@mail.med.upenn.edu) (L.P.),  
[evans@salk.edu](mailto:evans@salk.edu) (R.M.E.)

### In Brief

Neurons exclusively use glucose as fuel. Pei et al. show that the estrogen-related receptor gamma ( $ERR\gamma$ ) regulates a neural gene network promoting mitochondrial oxidative metabolism that is essential to meet the energy demand of spatial learning and memory formation.

### Highlights

- $ERR\gamma$  regulates oxidative glycolytic metabolism in neurons
- $ERR\gamma^{-/-}$  neurons exhibit decreased metabolic capacity
- LTP deficiency of  $ERR\gamma^{-/-}$  hippocampal slices is rescued by pyruvate
- Neuronal  $ERR\gamma$  knockouts impair spatial learning and memory

### Accession Numbers

GSE47135



# Dependence of Hippocampal Function on $ERR\gamma$ -Regulated Mitochondrial Metabolism

Liming Pei,<sup>1,\*</sup> Yangling Mu,<sup>2,8</sup> Mathias Leblanc,<sup>3</sup> William Alaynick,<sup>3</sup> Grant D. Barish,<sup>5</sup> Matthew Pankratz,<sup>3</sup> Tiffany W. Tseng,<sup>3</sup> Samantha Kaufman,<sup>3,4</sup> Christopher Liddle,<sup>6</sup> Ruth T. Yu,<sup>3</sup> Michael Downes,<sup>3</sup> Samuel L. Pfaff,<sup>3,4</sup> Johan Auwerx,<sup>7</sup> Fred H. Gage,<sup>2</sup> and Ronald M. Evans<sup>3,4,\*</sup>

<sup>1</sup>Center for Mitochondrial and Epigenomic Medicine, Department of Pathology and Laboratory Medicine, Children's Hospital of Philadelphia and Perelman School of Medicine, University of Pennsylvania, Philadelphia, PA 19104, USA

<sup>2</sup>Laboratory of Genetics

<sup>3</sup>Gene Expression Laboratory

<sup>4</sup>Howard Hughes Medical Institute

Salk Institute for Biological Studies, La Jolla, CA 92037, USA

<sup>5</sup>Division of Endocrinology, Metabolism, and Molecular Medicine, Department of Medicine, Feinberg School of Medicine, Northwestern University, Chicago, IL 60611, USA

<sup>6</sup>Storr Liver Unit, Westmead Millennium Institute and University of Sydney, Westmead Hospital, Westmead, New South Wales 2145, Australia

<sup>7</sup>Laboratory of Integrative and Systems Physiology, École Polytechnique Fédérale de Lausanne, 1015 Lausanne, Switzerland

<sup>8</sup>Present address: Department of Physiology, School of Basic Medicine and Institute of Brain Research, Huazhong University of Science and Technology, Wuhan 430030, China

\*Correspondence: [lpei@mail.med.upenn.edu](mailto:lpei@mail.med.upenn.edu) (L.P.), [evans@salk.edu](mailto:evans@salk.edu) (R.M.E.)

<http://dx.doi.org/10.1016/j.cmet.2015.03.004>

## SUMMARY

Neurons utilize mitochondrial oxidative phosphorylation (OxPhos) to generate energy essential for survival, function, and behavioral output. Unlike most cells that burn both fat and sugar, neurons only burn sugar. Despite its importance, how neurons meet the increased energy demands of complex behaviors such as learning and memory is poorly understood. Here we show that the estrogen-related receptor gamma ( $ERR\gamma$ ) orchestrates the expression of a distinct neural gene network promoting mitochondrial oxidative metabolism that reflects the extraordinary neuronal dependence on glucose.  $ERR\gamma^{-/-}$  neurons exhibit decreased metabolic capacity. Impairment of long-term potentiation (LTP) in  $ERR\gamma^{-/-}$  hippocampal slices can be fully rescued by the mitochondrial OxPhos substrate pyruvate, functionally linking the  $ERR\gamma$  knockout metabolic phenotype and memory formation. Consistent with this notion, mice lacking neuronal  $ERR\gamma$  in cerebral cortex and hippocampus exhibit defects in spatial learning and memory. These findings implicate neuronal  $ERR\gamma$  in the metabolic adaptations required for memory formation.

## INTRODUCTION

Mature neurons have exceedingly high energy demands, requiring a continuous supply of adenosine triphosphate (ATP) for survival, excitability, as well as for the synaptic signaling and circuitry underlying different behaviors. Neurons utilize aerobic metabolism of glucose, but not fat, to meet their fluctuating

needs (Escartin et al., 2006; Magistretti, 2003). Indeed, the predominance of pyruvate as the mitochondrial substrate for ATP generation suggests the possibility of a distinct neuronal mitochondrial phenotype. Defects in neuronal metabolism, especially in mitochondrial OxPhos, are associated with aging and diverse human neurological diseases (Lazarov et al., 2010; Mattson et al., 2008; Schon and Przedborski, 2011; Stoll et al., 2011; Wallace, 2005). In addition, neuronal metabolism (especially glucose uptake) and blood flow are tightly coupled with neuronal activity, an adaptation to the increased energy demand from complex tasks such as learning and memory (Howarth et al., 2012; Patel et al., 2004; Shulman et al., 2004). This neurometabolic and neurovascular coupling provides the basis for widely used brain imaging techniques including fMRI and positron emission tomography (Fox et al., 1988; Shulman et al., 2004). However, the molecular underpinnings regulating neuronal metabolism and its link to behavior remain poorly understood. Though such metabolic adaptations are at least partially mediated by transcriptional mechanisms that modulate the expression of metabolic genes (Alberini, 2009; Magistretti, 2006), the key transcription factors involved remain to be identified.

## RESULTS

### $ERR\gamma$ Is Highly Expressed in Both Developing and Mature Neurons

To investigate the global impact of metabolism on neuronal function and behavior, we aimed to identify key transcription factors that regulate metabolism in the neurons. Neuronal differentiation is known to induce mitochondrial biogenesis and OxPhos (Mattson et al., 2008). Therefore we reasoned that key neuronal metabolic regulators would be concordantly induced. We used a well-established protocol to differentiate mouse embryonic stem (ES) cells into neurons with high degree of uniformity (Bibel et al., 2007). We then examined the expression of some transcription

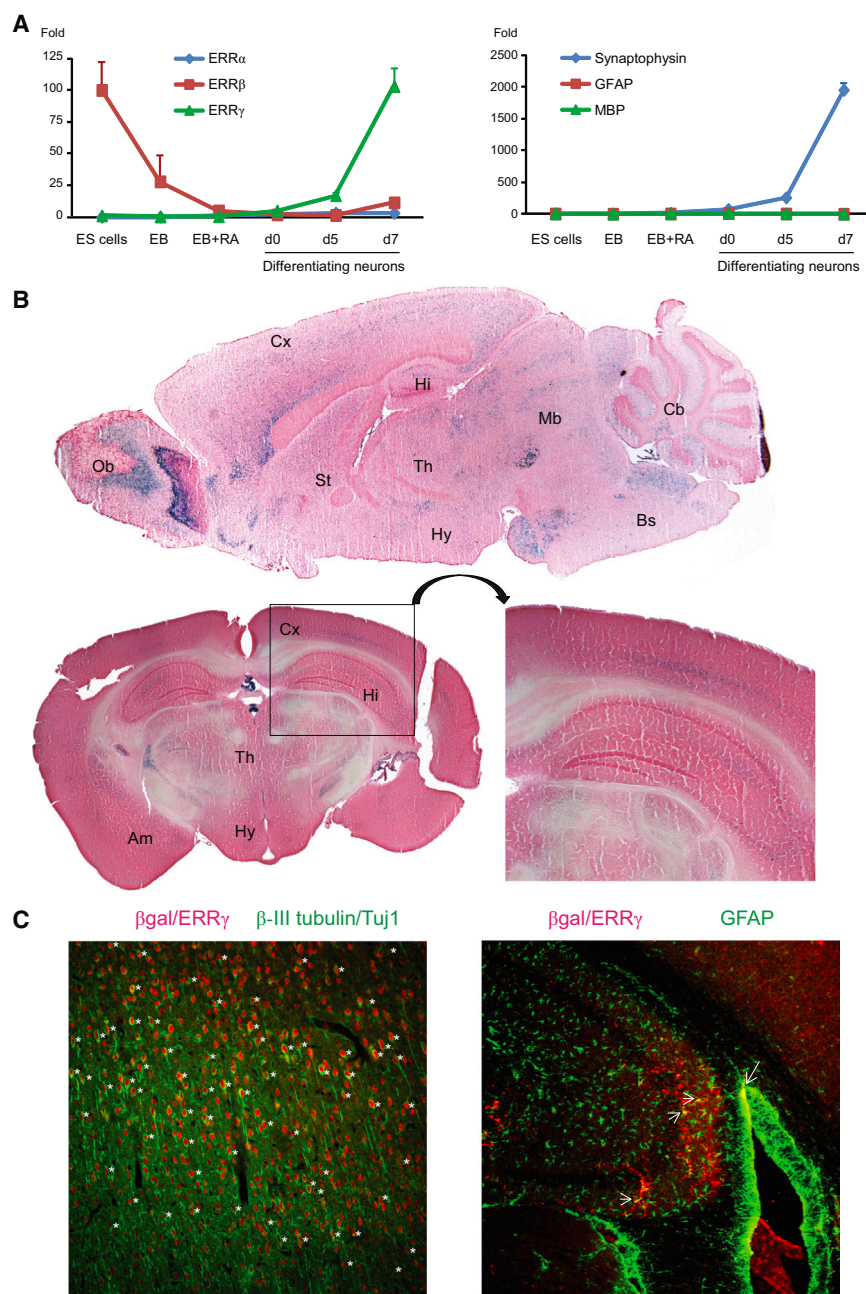


### Figure 1. ERR $\gamma$ Is Highly Expressed in Both Developing and Mature Neurons

(A) Expression of ERR $\alpha$ , ERR $\beta$ , ERR $\gamma$ , neuron marker synaptophysin, astrocyte marker GFAP, and oligodendrocyte marker MBP during mouse ES cell differentiation were measured using qRT-PCR. The y axis indicates fold change of gene expression compared to the ES cells (except for ERR $\beta$  where the ES cell level is set as 100). The result is presented as mean + SEM.

(B) ERR $\gamma$  expression pattern in the adult mouse brain was revealed via X-gal staining in 5-month-old female ERR $\gamma^{+/-}$  mice. Part of the cerebrum and hippocampus areas were enlarged for better visualization. Ob, olfactory bulb; Cx, cerebral cortex; Hi, hippocampus; Th, thalamus; Hy, hypothalamus; Mb, midbrain; Cb, cerebellum; St, striatum; Am, amygdala; Bs, brain stem.

(C) Immunostaining of  $\beta$ gal/ERR $\gamma$  and different cell type markers in 4-month-old ERR $\gamma^{+/-}$  mouse cerebrum and hippocampus reveals that ERR $\gamma$  is expressed in most neurons (indicated by asterisks next to the right side of the cell) and in some astrocytes (arrows). Please note that most neurons are ERR $\gamma$  positive, and only a portion of them are marked by asterisks.

factory bulb, cerebral cortex, hippocampus, thalamus, hypothalamus, midbrain, striatum, amygdala, and brain stem (Figure 1B). For example, many cells in the cerebral cortex, hippocampal CA, and dentate gyrus regions expressed ERR $\gamma$ . Co-immunostaining with different cell type markers suggested that most ERR $\gamma$ -expressing cells in the adult brain were neurons, though it was also expressed in some astrocytes (Figure 1C).

### ERR $\gamma$ Regulates Neuronal Metabolism

To elucidate a potential role for ERR $\gamma$  in regulating neuronal metabolism, we used chromatin immunoprecipitation followed by deep sequencing (ChIP-Seq) to map the genome-wide binding sites (cistrome) of ERR $\gamma$  in neurons. Notably,

factors with established metabolic regulatory function in peripheral tissues based on existing literature. We found that ERR $\gamma$  was highly induced during neuronal differentiation (Figure 1A). In contrast, ERR $\alpha$  expression was barely changed. ERR $\beta$  is highly expressed in ES cells and is one of the key factors for their maintenance (Feng et al., 2009); its expression was decreased during neuronal differentiation. Using a mouse strain where LacZ was inserted into the *Esrrg* locus, our previous work has shown that ERR $\gamma$  is highly expressed in the developing embryonic CNS in vivo as well (Alaynick et al., 2007). Consistent with previous reports using in situ hybridization (Gofflot et al., 2007; Lorke et al., 2000), X-gal staining revealed that ERR $\gamma$  protein was abundant and widely expressed in the adult mouse brain, including the ol-

an unusually high percentage of ERR $\gamma$  binding sites fell in the promoter regions (~36%), and the locations in intronic and intergenic regions were also significant (~28% and 30%, respectively) (Figure 2A). This tendency of ERR $\gamma$  to bind to the promoter regions may reflect its preference to associate with certain transcriptional co-factor or chromatin-remodeling complexes. Indeed, sequence motif analysis revealed an extensive colocalization of ERR $\gamma$  and nuclear respiratory factors (NRFs), established transcriptional regulators of nuclear genes encoding respiratory subunits, and components of the mitochondrial transcription and replication machinery (Figures 2B and S1A). Pathway analysis revealed that the most represented pathways were related to ATP generation, especially OxPhos (Figure S1B;

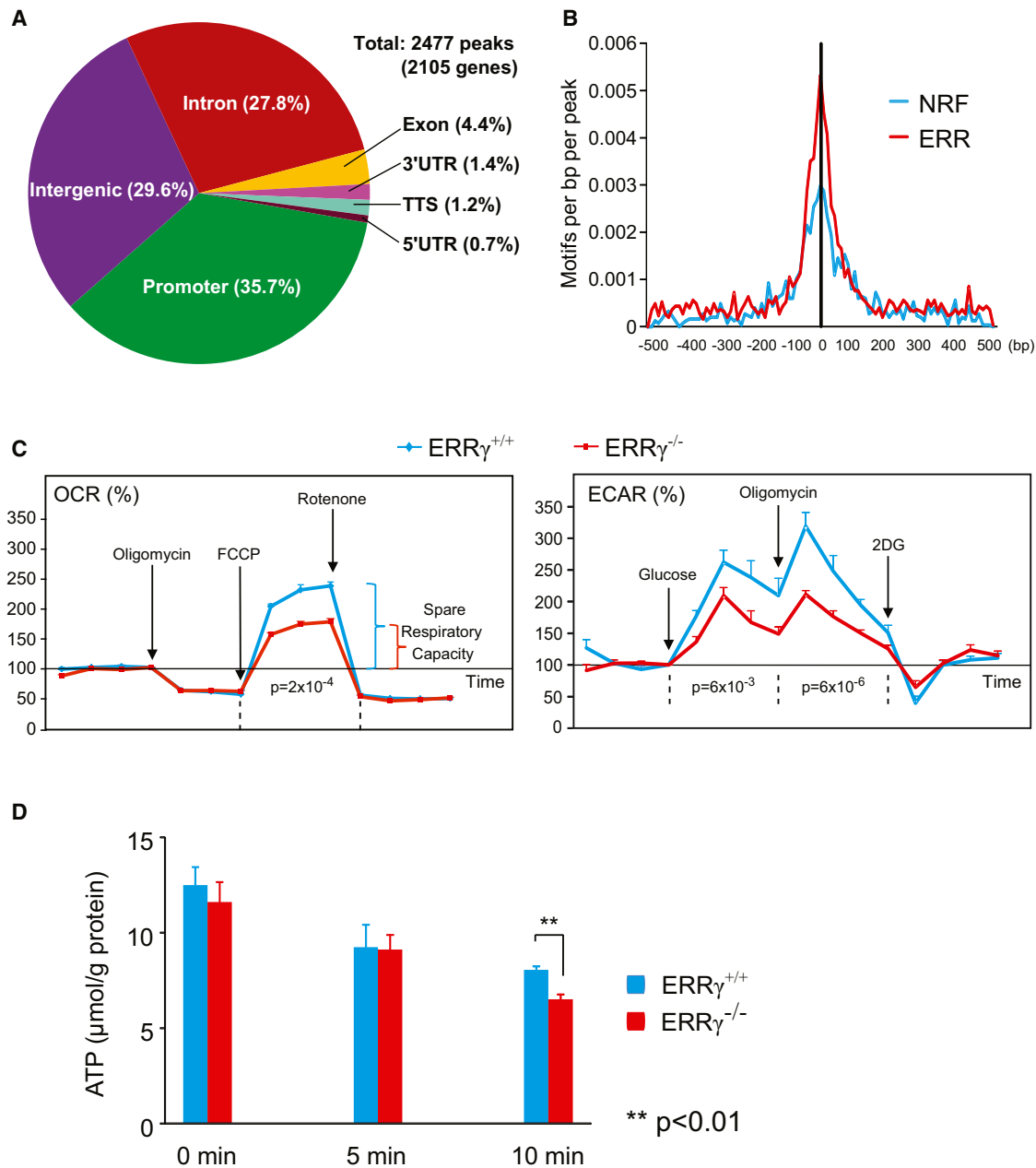


**Figure 2. ERR $\gamma$  Regulates Neuronal Metabolism**

(A) Pie chart shows the distribution of genome-wide ERR $\gamma$  binding sites revealed by ChIP-Seq.

(B) Histogram of motif densities near ERR $\gamma$  binding sites is shown. ERR and NRF motifs are graphed based on their distances to the center of ERR $\gamma$ -bound peaks.

(C) OCR and ECAR were measured in WT and ERR $\gamma$ <sup>-/-</sup> primary cortical neurons. Values were normalized to the baseline. The result is presented as mean + SEM. (n = 4). Two-factor with replication ANOVA using data points of each treatment was used to calculate and determine the statistical significance. FCCP, p-trifluorocarbonyl cyanide phenylhydrazide; 2DG, 2-deoxy-D-glucose. Drugs used were the following: 1  $\mu$ M oligomycin A, 4  $\mu$ M FCCP, and 2  $\mu$ M rotenone for OCR; 10 mM glucose, 2  $\mu$ M oligomycin A, and 100 mM 2DG for ECAR.

(D) The cellular ATP level in WT and ERR $\gamma$ <sup>-/-</sup> primary cortical neurons at different time points after 1  $\mu$ M FCCP treatment was measured and normalized to cellular protein level. The result is presented as mean + SEM. (n = 4). Two-tailed, unpaired, unequal variance t test was used to calculate and determine the statistical significance. See also Figure S1.

Table S1). For example, ChIP-Seq analysis revealed that ERR $\gamma$  bound to the promoter regions of genes important in transcriptional regulation (*Esrra*, *Gabpa/Nrf2a*, etc.), glycolysis (*Eno1*, *Gpi1*, *Pfkfb3*, *Ldhb*, etc.), TCA cycle (*Fh*, *Idh3a*, *Ogdh*, *Sdhb*,

etc.), OxPhos (*Cox5a*, *Cox6c*, *Cox8a*, *Atp5b*, etc.), and mitochondrial functions (*Mrp139*, *Tomm40*, *Slc25a4/Ant1*, *Mtch2*, etc.), which were confirmed by conventional ChIP (Figures S1C and S1D).



In contrast to previous ChIP-on-chip studies of ERR $\gamma$  in the mouse heart (Dufour et al., 2007), the neuronal ERR $\gamma$  cistrome was depleted of genes involved in fatty acid oxidation, an active process in cardiomyocytes, but not in neurons. This indicates a cell-type-specific role for ERR $\gamma$  in regulating cellular metabolism, and supports the notion of an ERR $\gamma$ -dependent neuronal mitochondrial phenotype. We also used microarray analysis to compare gene expression in the cerebral cortex from newborn wild-type (WT) and ERR $\gamma^{-/-}$  mice; the cerebral cortex comprises a relatively pure neuronal lineage at this stage compared to adult cortex. Among the 1,215 genes that were differentially expressed ( $p < 0.00001$ ), the most significantly represented pathways were related to ATP generation, especially OxPhos (Figure S1E), highly overlapping with the ChIP-Seq result (Figure S1B). Importantly, mitochondrial OxPhos activity was significantly decreased in ERR $\gamma^{-/-}$  mouse cortex, demonstrating the functional importance of ERR $\gamma$  in supporting neuronal oxidative metabolism (Figure S1F).

We next investigated whether the loss of ERR $\gamma$  would affect the metabolic properties of neurons. Cultured primary WT and ERR $\gamma^{-/-}$  cortical neurons were morphologically similar, established strong synaptic connections (data not shown), and retained comparable protein levels of neuronal markers PSD95 and MAP2 (Figure S1G). Subsequently, their relative rates of oxygen consumption (indicating mitochondrial OxPhos) and extracellular pH change (indicating anaerobic glycolysis) were compared in real time using a Seahorse extracellular flux (XF) analyzer. Although WT and ERR $\gamma^{-/-}$  cortical neurons had comparable basal metabolic rates (data not shown), ERR $\gamma^{-/-}$  neurons exhibited a significantly reduced maximal and spare oxidative capacity, as determined by use of mitochondrial uncoupler FCCP to stimulate the maximal OxPhos rates (Figures 2C and S1H). ERR $\gamma^{-/-}$  neurons demonstrated only ~50% of the spare respiratory capacity of WT neurons, suggesting that ERR $\gamma$  was critical to achieve peak capacity for ATP production. ERR $\gamma^{-/-}$  neurons also displayed significantly decreased maximal glycolytic capacity when stimulated with glucose or ATP synthase inhibitor oligomycin A (Figure 2C). Accordingly, ERR $\gamma^{-/-}$  neurons exhibited an impaired ability to maintain their cellular ATP level (Figure 2D). Neither ERR $\gamma^{+/+}$  nor ERR $\gamma^{-/-}$  neurons increased their oxygen uptake in response to palmitate treatment, indicating that neurons' reliance on glucose, but not fat, as fuel was ERR $\gamma$  independent (Figure S1I). In addition, the dependence on ERR $\gamma$  for maximal metabolic capacity was cell-type-specific. Mouse embryonic fibroblasts (MEFs) express both ERR $\alpha$  and ERR $\gamma$  abundantly; however, loss of ERR $\gamma$  did not affect their total oxidative and glycolytic capacity (Figure S1J).

### ERR $\gamma$ Deletion Significantly Impairs Hippocampal LTP, which Is Rescued by Mitochondrial OxPhos Substrate Pyruvate

We next sought to evaluate the in vivo importance of ERR $\gamma$ -regulated neuronal metabolism in energy-demanding brain functions such as learning and memory. Since ERR $\gamma^{-/-}$  mice die within days of birth (Alaynick et al., 2007), floxed ERR $\gamma$  alleles were targeted with a late-onset neuron-specific enolase-cre (NSE or Eno2-Cre), to generate mature neuron ERR $\gamma$  knockout (KO) mice (Figure S2A). Crosses with a Tomato/GFP reporter line (Muzumdar et al., 2007) confirmed that Eno2-Cre yielded a strong,

high-percentage recombination in cerebral cortex, hippocampus, part of the olfactory bulb, thalamus, and brain stem, but only sporadically in other brain regions (Figure S2B). By comparing this recombination pattern with the endogenous ERR $\gamma$  expression pattern (Figure 1B) to subtract non-ERR $\gamma$ -expressing areas, we found that Eno2-Cre resulted in efficient deletion of ERR $\gamma$  in the cerebral cortex, hippocampus, and partial olfactory bulb. ERR $\gamma$  deficiency in these regions was confirmed by quantifying both the mRNA and nuclear protein levels of ERR $\gamma$  (Figure S2C). The residual ERR $\gamma$  may be due to incomplete neuronal deletion or exist because ERR $\gamma$  is also expressed in non-neuronal cells (Figure 1C). These neuronal ERR $\gamma$  KO mice were born in a Mendelian ratio and appeared grossly normal. Both male and female mice had body weights similar to Cre-controls (Figure S2D). We evaluated their brain morphology via Nissl staining. Detailed comparison of the coronal sections at different planes revealed normal histology. In particular, all the structural features and nuclei were present and microscopically normal (Figure S2E). Electron microscopy revealed that neuronal ERR $\gamma$  KO mouse hippocampi possessed normal subcellular structure, mitochondrial morphology, and synaptic vesicles (Figure S2F; data not shown), and no significant differences were seen in the levels of the neurotransmitter glutamate across several brain regions (Figure S2G). Most importantly, the neuronal ERR $\gamma$  KO mouse hippocampi exhibited normal baseline electrophysiological properties as measured by input-output function and paired pulse ratio (PPR; Figures 3A and 3B), suggesting that the basal hippocampal synaptic transmission and circuits were functional and not affected by loss of ERR $\gamma$ .

LTP is well established as a key neuronal mechanism that underlies learning and memory (Bliss and Collingridge, 1993; Kelleher et al., 2004). The ability of neurons to appropriately enhance synaptic transmission through a memory-generating experience depends upon an abundant energy source for ATP-dependent action potentials as well as cycles of neurotransmitter synthesis, release, reuptake, and recycling (Bélanger et al., 2011). We therefore next recorded hippocampal CA1 LTP (field excitatory post-synaptic potential, fEPSP) in brain slices from these mice. The baseline response was comparable between control and neuronal ERR $\gamma$  KO mice, again suggesting intact neuronal connections and excitability. However, there was a significant reduction of CA1 LTP in the neuronal ERR $\gamma$  KO mice (Figures 3C and 3D). In fact, these mice exhibited LTP barely above baseline after stimulation. To determine whether the observed defect in LTP was caused by a metabolic deficiency, we supplemented the hippocampal slices with pyruvate, a well-known energy source and mitochondrial OxPhos substrate, during LTP measurements. Addition of pyruvate should increase the metabolic flux rate of OxPhos and therefore enhance ATP generation. Remarkably, pyruvate supplementation completely rescued the LTP defects in neuronal ERR $\gamma$  KO, but had no effect on control hippocampal slices (Figures 3C and 3D), establishing a causal link between the metabolic deficiency and the LTP defects.

### Loss of Neuronal ERR $\gamma$ In Vivo Impairs Spatial Learning and Memory

We next investigated whether loss of cortical and hippocampal neuronal ERR $\gamma$  impacted in vivo animal behavior, in particular, hippocampal-dependent spatial learning and memory. As

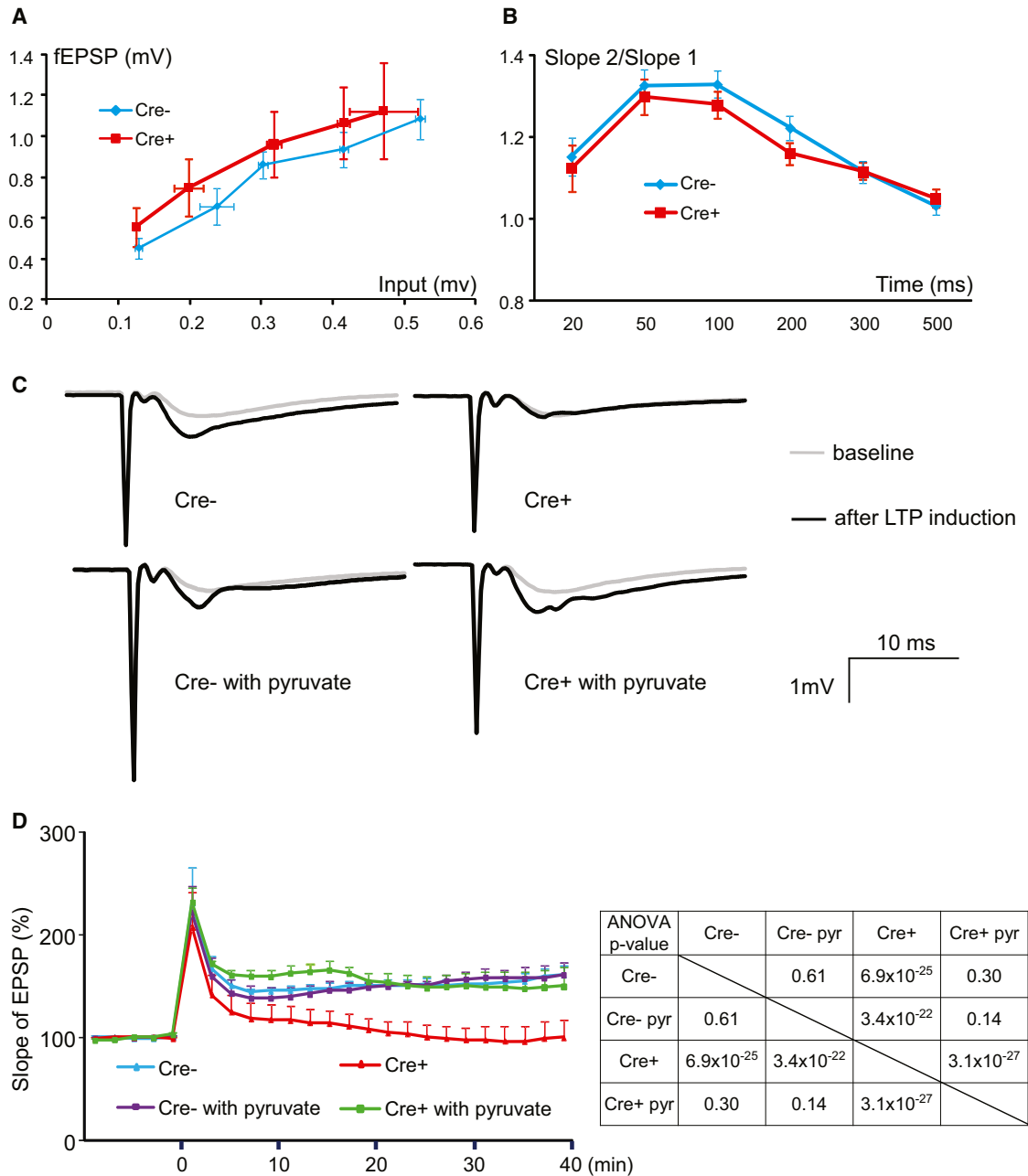


### Figure 3. $ERR\gamma$ Deletion Significantly Impairs Hippocampal LTP, which Is Rescued by Mitochondrial OxPhos Substrate Pyruvate

(A and B) Input-output function (A) and PPR (B) were measured in 5- to 6-month-old Cre<sup>-</sup> and Cre<sup>+</sup> mouse hippocampal slices. The result is presented as mean  $\pm$  SEM. (C) Sample traces of 5- to 6-month-old Cre<sup>-</sup> and Cre<sup>+</sup> mouse hippocampal CA1 LTP with or without 2.5 mM pyruvate.

(D) Cre<sup>-</sup> and Cre<sup>+</sup> mouse hippocampal CA1 LTP (slope of fEPSP) with or without 2.5 mM pyruvate. The result is presented as mean  $\pm$  SEM. (n = 6). Two-factor with replication ANOVA was used to calculate and determine the statistical significance. p value from ANOVA is shown in the insert table. See also Figure S2.

$ERR\gamma$  expression appeared intact in most other brain regions, we did not expect that the behaviors heavily dependent on other brain areas would be affected. The functional observational battery (Crawley, 2000) showed normal sensory perception, motor control, and reflexes. Metabolic cage studies revealed a normal circadian pattern of movement (Figure S3A) and normal respiratory exchange ratio (RER; Figure S3B). Furthermore, a series of behavioral tests revealed that the neuronal  $ERR\gamma$  KO mice had

normal vision (visual cliff test, data not shown), motor coordination and balance (rotarod test, Figure S3C), exploratory activity (open field test, Figure S3D), and anxiety (light/dark box test, Figure S3E; and elevated plus maze test, Figure S3F). In sharp contrast, these mice exhibited severe defects in spatial learning and memory in the Morris water maze test compared to control Cre<sup>-</sup> mice (Figures 4A, 4B, and S3G). Although they had no problem locating a visible platform in the Morris water maze indicating

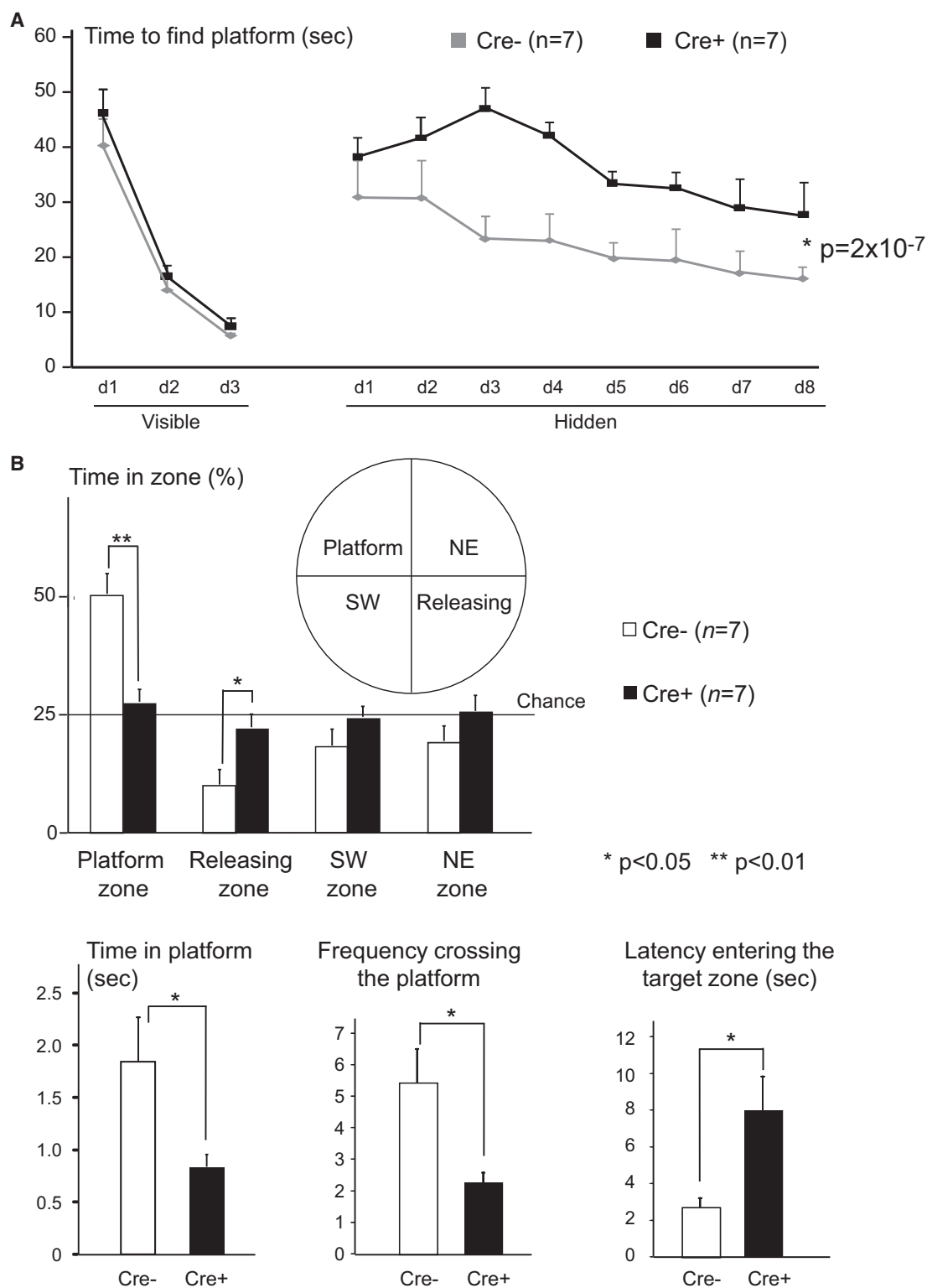


#### Figure 4. Loss of Neuronal $ERR\gamma$ In Vivo Impairs Spatial Learning and Memory

(A) The learning curves of 4-month-old Cre<sup>-</sup> and Cre<sup>+</sup> mice in finding visual or hidden platform in the Morris water maze test. The result is presented as mean + SEM. Two-factor with replication ANOVA was used to calculate and determine the statistical significance.

(B) Spatial memory was evaluated using a probe test in the Morris water maze. Time spent in different zones/platform, frequency crossing the platform, and the latency in entering the target zone are shown. The result is presented as mean + SEM. Two-tailed, unpaired, unequal variance t test was used to calculate and determine the statistical significance. See also Figure S3.

normal vision and swimming ability, they were significantly slower in learning to locate the hidden platform (Figure 4A). They also exhibited significantly poorer memory in the probe test to locate the original position of the removed platform (less time spent swimming in the platform zone, less frequency crossing the platform, and longer latency to first enter the target zone; Figure 4B).

## DISCUSSION

Our studies here identify an essential role for ERR $\gamma$  in the regulation of neuronal metabolism required for spatial learning and memory. Mechanistically, we identify an ERR $\gamma$  genomic signature in neurons consistent with their utilization of glucose, but not fat, in mitochondrial OxPhos and energy generation. This neuronal ERR $\gamma$  genomic signature, combined with the marked reduction in spare respiratory capacity of neurons lacking ERR $\gamma$ , suggests that persistent synaptic changes associated with memory formation may be limited by insufficient energy in neuronal ERR $\gamma$  KO mice. Indeed, the finding that LTP defects in neuronal ERR $\gamma$  KO hippocampus were rescued by pyruvate supplementation supports a role for ERR $\gamma$  in regulating neuronal metabolism. Consistent with this notion, mice lacking neuronal ERR $\gamma$  exhibited defects in spatial learning and memory. As ERR $\gamma$  activity can be modulated with small molecules, targeting ERR $\gamma$ -dependent neuronal metabolic pathways could provide new therapeutic avenues in the clinical treatment of a variety of neurological diseases.

In addition to ERR $\gamma$ , closely related proteins ERR $\alpha$  and ERR $\beta$  have been shown as important transcriptional regulators of cellular metabolism in peripheral tissues. The three ERR proteins clearly have non-overlapping functions, since the individual ERR KO mouse exhibits different phenotypes (Alaynick et al., 2007; Luo et al., 1997, 2003). On the other hand they bind to overlapping loci in the genome, as illustrated in the mouse heart for ERR $\alpha$  and ERR $\gamma$  (Dufour et al., 2007). Our current and previous studies as well as data from the Allen Brain Atlas indicate that all three ERR proteins are expressed in the brain, but with distinct time and spatial patterns (Gofflot et al., 2007; Lorke et al., 2000; Real et al., 2008). For example, ERR $\beta$  is primarily expressed in the developing brain, and ERR $\alpha$  expression pattern in the adult brain is more ubiquitous compared to ERR $\beta$  and ERR $\gamma$ . This is significant because different brain cell types (neurons, astrocytes, oligodendrocytes, etc.) and same cell types in different brain regions and during different developmental stages exhibit diverse metabolic properties (Fünfschilling et al., 2012; Goyal et al., 2014; Vilchez et al., 2007). The nature and importance of these differences and how such differential metabolic regulation is achieved remain poorly understood. Our current study reveals that ERR $\gamma$  is essential for metabolism and learning/memory of the mature neurons in the hippocampus. Future studies are needed to determine whether the three ERR proteins regulate distinct cellular metabolism, functions, and related behaviors in different cell types, brain regions, and developmental stages.

## EXPERIMENTAL PROCEDURES

### Animal Experiments

All animal procedures were approved by and carried out under the guidelines of the Institutional Animal Care and Use Committees of the Salk Institute and the Children's Hospital of Philadelphia. All mice were maintained in a temper-

ature- and light-controlled (6am–6pm light) environment and received a standard diet (PMI laboratory rodent diet 5001, Harlan Teklad) unless otherwise noted. ERR $\gamma$  KO mice were previously described (Alaynick et al., 2007), and heterozygous mice were backcrossed to C57BL6/J background for at least ten generations. The ERR $\gamma$  floxed and conditional KO strains were backcrossed to C57BL6/J background for at least six generations. Age- and gender-matched mice were used for all experiments.

### Gene Expression and Protein Analysis

RNA isolation, gene expression analysis by qRT-PCR, and western blot were performed as previously described (Pei et al., 2006).

### Histology, Immunofluorescence, and X-Gal Staining

Histological analysis and immunofluorescence were performed as previously described (Pei et al., 2011).

### Isolation and Culture of MEFs

The isolation and culture of MEFs were performed as previously described (Pei et al., 2011). MEFs within three generations of culture were used for the experiments.

### XF Analysis

We analyzed the bioenergetic profiles of ERR $\gamma$  WT and KO cells using XF24 XF analyzer (Seahorse Bioscience) following the manufacturer's protocol.

### Generation of ES Cell-Derived Neurons

We obtained the mouse ES cell line ES-D3 from American Type Culture Collection. We followed a previously published protocol (Bibel et al., 2007) to differentiate ES-D3 cells into homogeneous populations of glutamatergic neurons.

### ChIP-Seq

We fixed ES cell-derived neurons and performed ChIP-Seq as previously described (Pei et al., 2011).

### Microarray Analysis

RNA from WT and ERR $\gamma$  KO P0 cortex (technical duplicates of four cortices of each genotype) were extracted, and their purity was assessed by Agilent Technologies Bioanalyzer 2100. Microarray was performed as previously described (Pei et al., 2011).

### Neurotransmitter Analysis

Different brain regions were carefully dissected from 5-month-old control (Cre $-$ ) and neuronal ERR $\gamma$  KO (Cre $+$ ) littermates, weighed, and then grinded and lysed in hypotonic buffer containing proteinase inhibitors (Roche). Glutamate level in the lysates of individual samples was measured using a Sigma kit following the manufacturer's instructions and normalized to the sample weight.

### Mitochondrial Enzyme Activity

WT and ERR $\gamma$  KO P0 littermate mouse cortices were dissected, weighed, and homogenized in 20 volume (v/w) of homogenization buffer (1 mM EDTA and 50 mM triethanolamine in water) on ice. Complex III (Q-cytochrome c oxidoreductase) and Complex IV (cytochrome c oxidase) enzymatic activities were determined by the change in absorbance of cytochrome c measured at 550 nm. Assays were performed in 96-well plates with the "Kinetic" function of a SpectraMax Paradigm Multi-Mode Microplate Detection Platform (Molecular Devices). The linear slopes ( $\Delta$ OD/min) were calculated. The enzymatic activity was determined by the slope ( $\Delta$ OD/min)/cortex weight (mg)/molar extinction coefficient (OD/mmol/cm)/0.625 cm. The molar extinction coefficient for cytochrome c used was 29.5 OD/mmol/cm.

### Electrophysiology

Electrophysiology studies were performed using 5- to 6-month-old control and neuronal ERR $\gamma$  KO littermates as previously described with slight modification (Mu et al., 2011).

### Behavior Tests

All behavior tests were performed between 1pm and 6pm unless otherwise noted. We conducted metabolic and behavioral studies in mice without prior



drug administration or surgery in the following order: metabolic cages, rotarod, open field, light/dark box, elevated plus maze, and Morris water maze. We started the test with 2- to 4-month-old mice; they reached 5–6 months of age when the Morris water maze test was completed. All tests were repeated in 2–3 separate cohorts of mice, and similar results were observed. All behavioral studies were repeated by more than one investigator to assure the reproducibility.

### Statistical Analysis

Two-tailed, unpaired, unequal variance t test or two-factor with replication ANOVA (Microsoft Excel) were used to calculate and determine the statistical significance, with the criterion for significance set at  $p < 0.05$ . All figure error bars indicate SEM.

Please see the [Supplemental Information](#) for detailed experimental procedures.

### ACCESSION NUMBERS

The GEO accession number for the ChIP-Seq and microarray data reported in this paper is GSE47135.

### SUPPLEMENTAL INFORMATION

Supplemental Information includes three figures, two tables, and Supplemental Experimental Procedures and can be found with this article online at <http://dx.doi.org/10.1016/j.cmet.2015.03.004>.

### ACKNOWLEDGMENTS

We thank C. McDonald, M. Karunasiri, H. Juguilon, S. Andrews, M. Joens, and J. Fitzpatrick for technical and EM studies support; D. Wallace, A. Atkins, C. Perez-Garcia, R. Carney, W. Fan, J. Whyte, O. Chivatakarn, A. Levine, K. Hilde, T. Wang, R. Hernandez, Y. Kim, and M. Marchetto for helpful discussions; Z. Zhou for the PSD95 antibody; and E. Ong, C. Brondos, and S. Ganley for administrative assistance. R.M.E. is an investigator of the Howard Hughes Medical Institute at the Salk Institute for Biological Studies and March of Dimes Chair in Molecular and Developmental Biology. This work was supported by the Howard Hughes Medical Institute; NIH grants DK057978, HL105278, DK090962, and CA014195 (R.M.E.); NIMH MH090258 (F.H.G.); the Leona M. and Harry B. Helmsley Charitable Trust Grant (R.M.E. and F.H.G.); Ellison Medical Foundation (R.M.E.); Glenn Foundation for Medical Research (R.M.E.); the G. Harold & Leila Y. Mathers Charitable Foundation (F.H.G.); the JPB Foundation (F.H.G.); Annette Merrill-Smith (F.H.G.); pilot funds from the Research Institute of the Children's Hospital of Philadelphia (CHOP); CHOP Metabolism, Nutrition and Development Research Affinity Group Pilot Grant; and Penn Medicine Neuroscience Center (PMNC) Innovative Pilot Funding Program (L.P.). L.P. conceived of the project and designed and performed most of the experiments. Y.M. performed the hippocampal LTP recordings and analyzed the data together with L.P. M.L. is a pathologist who evaluated the histology and staining results. W.A. performed some of the X-gal staining and immunostaining experiments. R.T.Y. and C.L. analyzed the ChIP-Seq and microarray data. G.D.B., M.P., T.W.T., S.K., M.D., S.L.P., and J.A. provided technical assistance, research materials, or intellectual input. R.M.E. supervised the project. L.P. and R.M.E. wrote, and F.H.G., M.D., and R.T.Y. reviewed and edited, the manuscript. L.P., R.T.Y., M.D., and R.M.E. are coinventors of a method of modulating hippocampal function and may be entitled to royalties.

Received: March 14, 2014

Revised: January 16, 2015

Accepted: February 27, 2015

Published: April 7, 2015

### REFERENCES

Alaynick, W.A., Kondo, R.P., Xie, W., He, W., Dufour, C.R., Downes, M., Jonker, J.W., Giles, W., Naviaux, R.K., Giguère, V., and Evans, R.M. (2007).

ERRgamma directs and maintains the transition to oxidative metabolism in the postnatal heart. *Cell Metab.* 6, 13–24.

Alberini, C.M. (2009). Transcription factors in long-term memory and synaptic plasticity. *Physiol. Rev.* 89, 121–145.

Bélanger, M., Allaman, I., and Magistretti, P.J. (2011). Brain energy metabolism: focus on astrocyte-neuron metabolic cooperation. *Cell Metab.* 14, 724–738.

Bibel, M., Richter, J., Lacroix, E., and Barde, Y.A. (2007). Generation of a defined and uniform population of CNS progenitors and neurons from mouse embryonic stem cells. *Nat. Protoc.* 2, 1034–1043.

Bliss, T.V., and Collingridge, G.L. (1993). A synaptic model of memory: long-term potentiation in the hippocampus. *Nature* 361, 31–39.

Crawley, J.N. (2000). What's Wrong with my Mouse?: Behavioral Phenotyping of Transgenic and Knockout Mice. (Wiley-Liss).

Dufour, C.R., Wilson, B.J., Huss, J.M., Kelly, D.P., Alaynick, W.A., Downes, M., Evans, R.M., Blanchette, M., and Giguère, V. (2007). Genome-wide orchestration of cardiac functions by the orphan nuclear receptors ERRalpha and gamma. *Cell Metab.* 5, 345–356.

Escartin, C., Valette, J., Lebon, V., and Bonvento, G. (2006). Neuron-astrocyte interactions in the regulation of brain energy metabolism: a focus on NMR spectroscopy. *J. Neurochem.* 99, 393–401.

Feng, B., Jiang, J., Kraus, P., Ng, J.H., Heng, J.C., Chan, Y.S., Yaw, L.P., Zhang, W., Loh, Y.H., Han, J., et al. (2009). Reprogramming of fibroblasts into induced pluripotent stem cells with orphan nuclear receptor Esrrb. *Nat. Cell Biol.* 11, 197–203.

Fox, P.T., Raichle, M.E., Mintun, M.A., and Dence, C. (1988). Nonoxidative glucose consumption during focal physiologic neural activity. *Science* 241, 462–464.

Fünfschilling, U., Supplie, L.M., Mahad, D., Boretius, S., Saab, A.S., Edgar, J., Brinkmann, B.G., Kassmann, C.M., Tzvetanova, I.D., Möbius, W., et al. (2012). Glycolytic oligodendrocytes maintain myelin and long-term axonal integrity. *Nature* 485, 517–521.

Gofflot, F., Chartoire, N., Vasseur, L., Heikkinen, S., Dembele, D., Le Merrer, J., and Auwerx, J. (2007). Systematic gene expression mapping clusters nuclear receptors according to their function in the brain. *Cell* 131, 405–418.

Goyal, M.S., Hawrylycz, M., Miller, J.A., Snyder, A.Z., and Raichle, M.E. (2014). Aerobic glycolysis in the human brain is associated with development and neonatal gene expression. *Cell Metab.* 19, 49–57.

Howarth, C., Gleeson, P., and Attwell, D. (2012). Updated energy budgets for neural computation in the neocortex and cerebellum. *J. Cereb. Blood Flow Metab.* 32, 1222–1232.

Kelleher, R.J., 3rd, Govindarajan, A., and Tonegawa, S. (2004). Translational regulatory mechanisms in persistent forms of synaptic plasticity. *Neuron* 44, 59–73.

Lazarov, O., Mattson, M.P., Peterson, D.A., Pimplikar, S.W., and van Praag, H. (2010). When neurogenesis encounters aging and disease. *Trends Neurosci.* 33, 569–579.

Lorke, D.E., Süssens, U., Borgmeyer, U., and Hermans-Borgmeyer, I. (2000). Differential expression of the estrogen receptor-related receptor gamma in the mouse brain. *Brain Res. Mol. Brain Res.* 77, 277–280.

Luo, J., Sladek, R., Bader, J.A., Matthysen, A., Rossant, J., and Giguère, V. (1997). Placental abnormalities in mouse embryos lacking the orphan nuclear receptor ERR-beta. *Nature* 388, 778–782.

Luo, J., Sladek, R., Carrier, J., Bader, J.A., Richard, D., and Giguère, V. (2003). Reduced fat mass in mice lacking orphan nuclear receptor estrogen-related receptor alpha. *Mol. Cell. Biol.* 23, 7947–7956.

Magistretti, P. (2003). Brain energy metabolism. In *Fundamental Neuroscience, Second Edition* (Academic Press), pp. 339–360.

Magistretti, P.J. (2006). Neuron-glia metabolic coupling and plasticity. *J. Exp. Biol.* 209, 2304–2311.

Mattson, M.P., Gleichmann, M., and Cheng, A. (2008). Mitochondria in neuroplasticity and neurological disorders. *Neuron* 60, 748–766.

- Mu, Y., Zhao, C., and Gage, F.H. (2011). Dopaminergic modulation of cortical inputs during maturation of adult-born dentate granule cells. *J. Neurosci.* *31*, 4113–4123.
- Muzumdar, M.D., Tasic, B., Miyamichi, K., Li, L., and Luo, L. (2007). A global double-fluorescent Cre reporter mouse. *Genesis* *45*, 593–605.
- Patel, A.B., de Graaf, R.A., Mason, G.F., Kanamatsu, T., Rothman, D.L., Shulman, R.G., and Behar, K.L. (2004). Glutamatergic neurotransmission and neuronal glucose oxidation are coupled during intense neuronal activation. *J. Cereb. Blood Flow Metab.* *24*, 972–985.
- Pei, L., Waki, H., Vaitheesvaran, B., Wilpitz, D.C., Kurland, I.J., and Tontonoz, P. (2006). NR4A orphan nuclear receptors are transcriptional regulators of hepatic glucose metabolism. *Nat. Med.* *12*, 1048–1055.
- Pei, L., Leblanc, M., Barish, G., Atkins, A., Nofsinger, R., Whyte, J., Gold, D., He, M., Kawamura, K., Li, H.R., et al. (2011). Thyroid hormone receptor repression is linked to type I pneumocyte-associated respiratory distress syndrome. *Nat. Med.* *17*, 1466–1472.
- Real, M.A., Heredia, R., Dávila, J.C., and Guirado, S. (2008). Efferent retinal projections visualized by immunohistochemical detection of the estrogen-related receptor beta in the postnatal and adult mouse brain. *Neurosci. Lett.* *438*, 48–53.
- Schon, E.A., and Przedborski, S. (2011). Mitochondria: the next (neurode)generation. *Neuron* *70*, 1033–1053.
- Shulman, R.G., Rothman, D.L., Behar, K.L., and Hyder, F. (2004). Energetic basis of brain activity: implications for neuroimaging. *Trends Neurosci.* *27*, 489–495.
- Stoll, E.A., Cheung, W., Mikheev, A.M., Sweet, I.R., Bielas, J.H., Zhang, J., Rostomily, R.C., and Horner, P.J. (2011). Aging neural progenitor cells have decreased mitochondrial content and lower oxidative metabolism. *J. Biol. Chem.* *286*, 38592–38601.
- Vilchez, D., Ros, S., Cifuentes, D., Pujadas, L., Vallès, J., García-Fojeda, B., Criado-García, O., Fernández-Sánchez, E., Medraño-Fernández, I., Domínguez, J., et al. (2007). Mechanism suppressing glycogen synthesis in neurons and its demise in progressive myoclonus epilepsy. *Nat. Neurosci.* *10*, 1407–1413.
- Wallace, D.C. (2005). A mitochondrial paradigm of metabolic and degenerative diseases, aging, and cancer: a dawn for evolutionary medicine. *Annu. Rev. Genet.* *39*, 359–407.